Supporting Information

Modulating Anion-Enriched Zn^{2+} Solvation Structure via Dual-Weak-Interaction for Stable Zinc-Metal Batteries

Guimei Yao,[a] Weimin Gao,[e] Rongxian Wang,[a] Jing Xu,[b] Xianfa Rao,[a]* Bingjun Yang,[c]* Lingyang Liu,[d]* Bao Liu[b]*

a Key Laboratory of Power Battery and Materials, School of Materials Science and Engineering, Jiangxi University of Science and Technology, Ganzhou 341000, China.
b Automotive Engineering Research Institute, Jiangsu University, Zhenjiang 212013, China.
c Research Center of Resource Chemistry and Energy Materials, State Key Laboratory of Solid Lubrication, Lanzhou Institute of Chemical Physics, Chinese Academy of Sciences, Lanzhou 730000, China.
d Shandong Provincial Key Laboratory of Chemical Energy Storage and Novel Cell Technology, School of Chemistry and Chemical Engineering, Liaocheng University, Liaocheng 252059, China.
e Laboratory of Chemistry and Chemical Engineering, Northwest Normal University, Lanzhou 730070, China.

Corresponding authors.
*E-mail: raoxianfa@126.com, yangbj@licp.cas.cn, liulingy0425@163.com, liubao921@163.com

Experimental section

Materials. Zn foils (99.99%, thickness = 0.1 mm), Cu foil, Ti foil, zinc trifluoromethanesulfonate ($Zn(OTf)_2$, ALADDIN, 98.0%), 1,3-Dimethly-2-imidazolidinone (DMI, ALADDIN, 99.0%), Anhydrous ethanol, deionized water, Aniline(ANI, DAMAO, 99.5%), Hydrochloric acid (HCl, 36.0~38.0%), Ammonium persulfate ($(NH_4)_2S_2O_8$, Sinopharm Chemical Reagent Co., Ltd, 98.0%), Glass fiber separators (Whatman GF/A), Super P, Polytetrafluoroethylene (PTFE). All chemicals and reagents were analytical grade and used without further purification.

Preparation of electrolyte. The pure aqueous electrolyte (noted as ZFH) was prepared by dissolving 2M $Zn(OTf)_2$ salt in deionized water. The modified electrolyte (noted as ZFDH) were prepared by dissolving 2 M $Zn(OTf)_2$ in a mixture of DMI and H_2O (volume ratio: 4 : 1) under stirring. The pure 1,3-Dimethly-2-imidazolidinone solvent was noted as pure DMI.

Preparation of Polyaniline (PANI) cathode. PANI was prepared according to previous reports.[1] Typically, 0.365 mL of ANI monomer was added into 15 mL of 1 M HCl solution in an ice bath. After being stirred for 1 h, 5 mL of 1 M HCl solution containing 0.228 g of $(NH_4)_2S_2O_8$ was added into the ANI solution dropwise under stirring in an ice bath. The colorless solution gradually became dark green after a few mins. When the reaction is continued for 1 h, the sample obtained were washed with deionized water and ethanol, and then dried at 60°C overnight in a vacuum oven. PANI in the form of a dark green powder was thus obtained.

The PANI based cathode was prepared by mixing PANI with Super P and polytetrafluoroethylene (PTFE) with the weight ratio of 6:3:1. The above mixture was mixed with a certain dose of anhydrous ethanol to form a slurry. The slurry was coated onto a titanium mesh as the electrode. Then it was dried in a vacuum oven at 130℃ overnight. The average mass loading of PANI was 1-1.2 mg cm^{-2}.[2-4]

Characterizations

The Raman spectroscopy of various electrolytes electrolyte structure was obtained using LabRAM HR Evolution (HORIBA JY) with a laser wavelength of 532 nm. Fourier transform infrared spectroscopy (FTIR) of electrolytes were performed on a

Spotlight200i Frontier FTIR spectrometer (Perkinelmer), covering a wavenumber range of 650-4000 cm^{-1}. Crystalline structures of all samples were analyzed by X-ray diffraction (XRD) technique on a desktop X-ray diffractometer (Shimadzu 6100) with Cu Kα radiation within the 2θ range of 5-80° and a scanning rate of 2° min^{-1}.The morphologies of the Zn anode and microstructure of the synthesized PANI were observed by scanning electron microscope (SEM) (MIRA3 TESCAN SU-8020), operated at 10 kV and 10 mA. Surface compositions of samples were analyzed by X-ray photoelectron spectroscopy (XPS) on a ESCALAB 250Xi spectrometer (ThermoFisher Scientific). All of the binding energies were referenced to the C 1s peak (284.8 eV). The electrode samples were washed with anhydrous ethanol solvent to remove residual electrolyte before the XPS characterization.

Electrochemical Measurements

Zn//Zn symmetric cells, Zn//Cu asymmetric cells, SS//SS symmetric cells, Zn//SS asymmetric cells and Zn// PANI full batteries were assembled in the air using CR2032 coin cells. Glass fibre was used as the separator. The diameter of Glass fibre is 16 mm. The diameter of the Zn foil is 12 mm. The diameter of the Cu foil is 14 mm. The performances of assembled Zn//Zn, Zn//Cu and Zn//PANI batteries were collected by Land CT3002A battery test system. The Zn^{2+} plating/stripping CE was measured using Zn//Cu asymmetric cells with a cut-off charging voltage of 0.6 V. The cycling stability of Zn electrodes was measured by Zn//Zn symmetric cells. The Linear scan voltammetry (LSV), Cyclic voltammetry (CV), Chromoamperograms (CA), Tafel plots (Tafel) and Electrochemical impedance spectroscopy (EIS) were all tested on an electrochemical workstation (CHI660e, China). The LSV measurement were carried out on the Zn//SS asymmetric cells at a scan rate of 1 mV s^{-1}. The Tafel plots were measured in a three-electrode system, in which Zn foil as the working electrode, Pt as the counter electrode, and Ag/AgCl as the reference electrode. The voltage range of the corrosion Tafel plots was between -0.5 and -1.4 V at a scan rate of 1 mV s^{-1}. The CV curves were carried out on the Zn//Cu asymmetric cells in the voltage range of -0.2 V-0.6 V at a scan rate of 1 mV s^{-1}. The CA curves were measured using Zn//Zn symmetric

cells with a fixed overpotential of -150 mV over 200s. The Zn//PANI full batteries were tested in the voltage range of 0.4-1.4V and the specific capacities were calculated based on the mass of active materials in the PANI cathode. The CV curves of Zn//PANI full batteries was tested using an electrochemical workstation (Metrohm Autolab PGSTAT 302N) in the voltage range of 0.4-1.4 V at a scan rate 0.1 mV s^{-1}.

Measurement method of ionic conductivity

Ionic conductivities (σ) of the electrolytes were measured in SS//SS symmetric cells. The EIS was conducted in a frequency range of 100 kHz to 0.01 Hz with AC voltage amplitude of 5 mV. The ionic conductivity (σ) was modelled according to the following equation:

$$\sigma = \frac{L}{R \bullet A} \tag{1}$$

where L is the electrolyte membrane thickness, R is the resistance according to the EIS measurement, and A is the contact area between the SS and electrolyte membranes.

Measurement method of activation energy (E_a)

The activation energy (E_a) of the electrolytes was measured in Zn//Zn symmetric cells. The EIS was conducted in a frequency range of 100 kHz to 0.01 Hz with AC voltage amplitude of 5 mV at different temperatures. The activation energy (E_a) was modelled according to the following Arrhenius equation:

$$R_{ct}^{-1} = A\, exp\left(\frac{-E_a}{RT}\right) \tag{2}$$

where R_{ct} is the charge transfer resistance, A is the frequency factor, R is the gas constant, and T is the absolute temperature.

Measurement method of Zn^{2+} transfer number ($t_{Zn^{2+}}$)

The Zn^{2+} transfer number of ($t_{Zn^{2+}}$) of the electrolytes was measured in Zn//Zn symmetric cells. The EIS was conducted in a frequency range of 100 kHz to 0.01 Hz with AC voltage amplitude of 5 mV. The CA curves was conducted at constant voltage (10 mV) for 1000s. The Zn^{2+} transfer number ($t_{Zn^{2+}}$) was modelled according to the following Bruce-Vincent equation:

$$t_{Zn^{2+}} = \frac{I_s(\Delta V - I_0 R_0)}{I_0(\Delta V - I_s R_s)} \quad (3)$$

where I_0 is the initial current and I_s is the steady-state current, R_0 and R_s are the initial and steady-state charge transfer resistances, ΔV is the applied polarization voltage (10 mV), respectively.

Computational Details

Molecular Dynamics (MD) simulations were performed using FORCITE module with COMPASSII force field in Material Studio 8.0. Firstly, 195 $Zn(OTf)_2$, 725 DMI, and 1080 water molecules were packed into a 40 × 40 × 40 $Å^3$ box using the MS software to simulate the system of 2 M $Zn(OTf)_2$ dissolved into DMI:H_2O by a volume ratio of 4:1. After structure optimization, the equilibrium simulations running 2ns were performed in the NPT ensemble[5, 6] at constant pressure (1.0 atmosphere) and temperature (298 K) in the cubic box with periodic boundary conditions in three directions, which was long enough for system energy, temperature and solvent density reaching stable. Here, the time step used was 5fs. After reaching equilibrium state, MD simulations were run again in the NVT (T = 298 K) ensemble for 2ns using the Nose-Hoover thermostat, with simulation trajectories recorded every 200 steps.

The calculations of binding energy (BE) were performed using DMol3 package in Materials Studio8.0. The generalized gradient approximation (GGA) with Perdew-Burke-Ernzerhof (PBE) exchange-correlation function was used in the calculations. The vacuum slab was set to 10 Å to avoid the interaction between periodical images. A DND 4.4 basis sets were used for all atoms of the studied system, The force and energy convergence criterion were set to 0.004 Ha $Å^{-1}$ and $2*10^{-5}$ Ha, respectively. The binding energy (BE) is defined with the following equation:

$$BE = E_{Zn^{2+}-Solv} - E_{Zn^{2+}} - E_{Solv} \quad (4)$$

where $E_{Zn^{2+}-Solv}$, $E_{Zn^{2+}}$ and E_{Solv} are the total electronic energies of Zn^{2+} ion binds with a solvent molecule, Zn^{2+} ion, and solvent molecule, respectively.

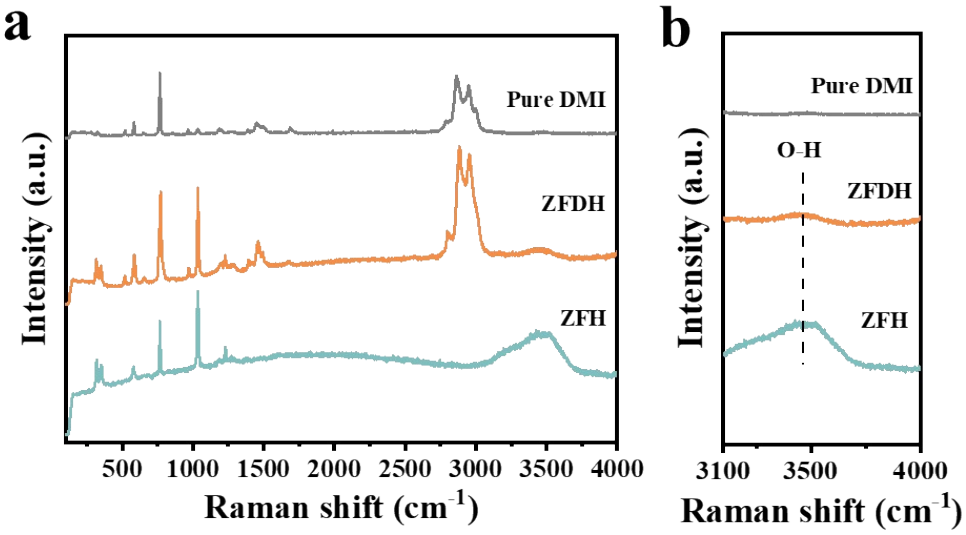

Fig. S1. Raman spectroscopy of pure DMI, ZFDH, and ZFH at (a)100-4000 cm^{-1} and (b)3100-4000 cm^{-1}.

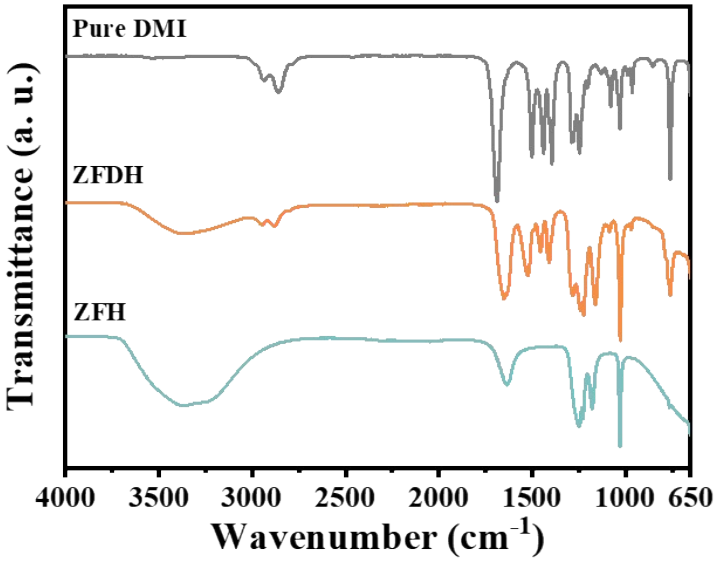

Fig. S2. FTIR spectroscopy of pure DMI, ZFDH, and ZFH at 650-4000 cm^{-1}.

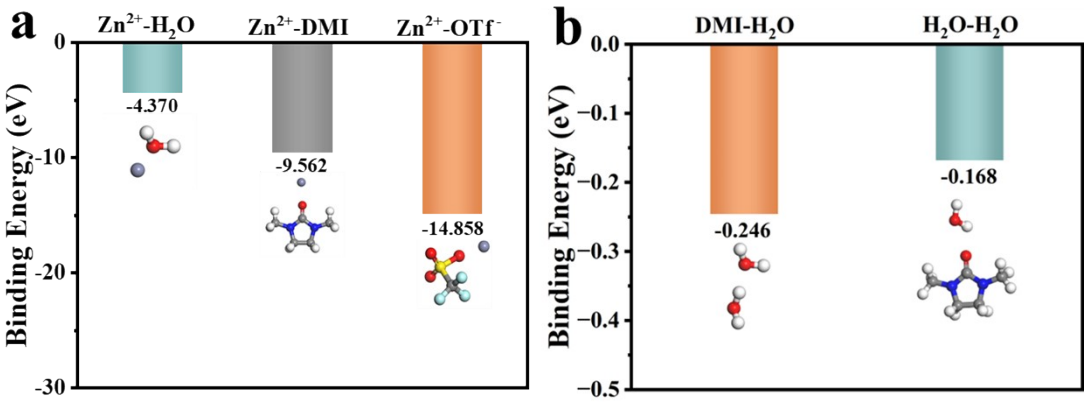

Fig. S3. The calculated binding energy of (a) Zn^{2+}-H_2O, Zn^{2+}-DMI and Zn^{2+}-OTf^- (b) DMI-H_2O, H_2O-H_2O.

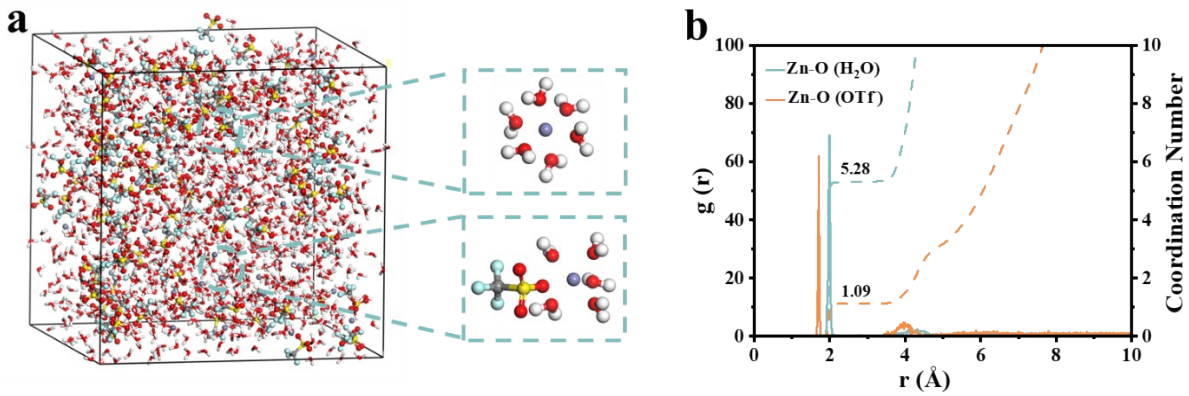

Fig. S4. (a)3D snapshots of the MD simulations for ZFH and schematics of Zn^{2+} solvent sheath. (b) RDFs and corresponding coordination numbers of Zn^{2+} in ZFH.

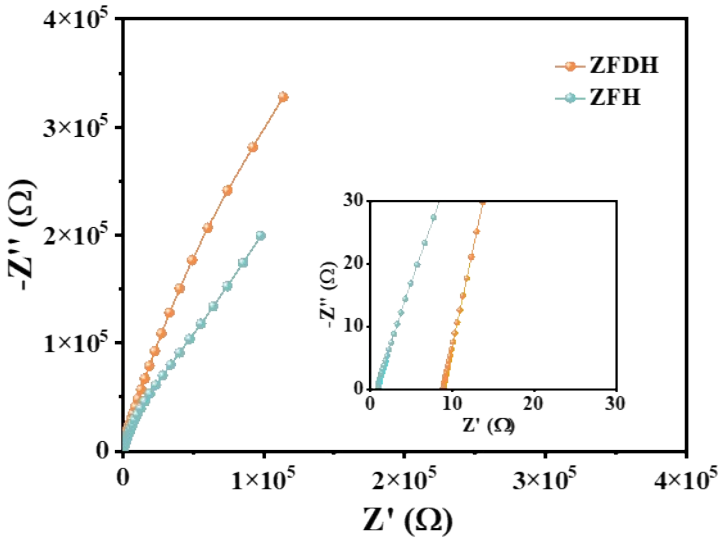

Fig. S5. Electrochemical impedance spectroscopy (EIS) curves of SS//SS cells in the ZFDH and ZFH electrolytes.

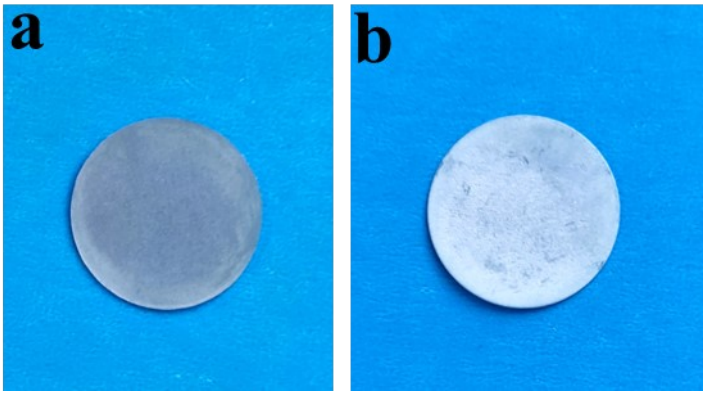

Fig. S6. Optical image of Zn metals being immersed in (a)ZFDH and (b)ZFH after 14 days.

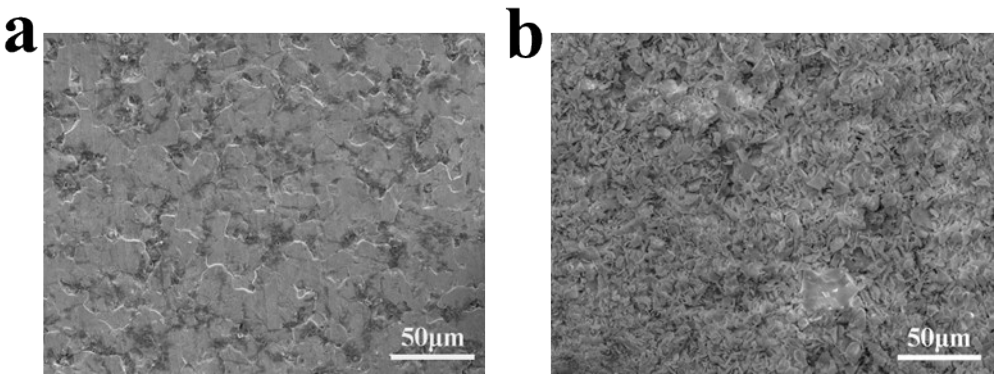

Fig. S7. SEM images of the Zn foil soaking for 14 days in the (a)ZFDH and (b)ZFH electrolyte.

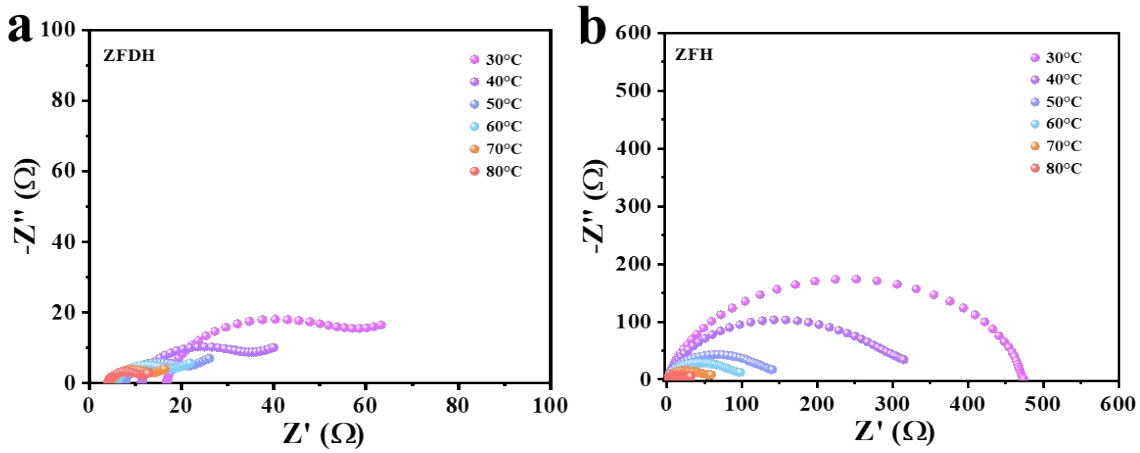

Fig. S8. Electrochemical impedance spectroscopy (EIS) curves of Zn//Zn symmetric cells in ZFDH (a) and ZFH (b) electrolytes under different temperatures.

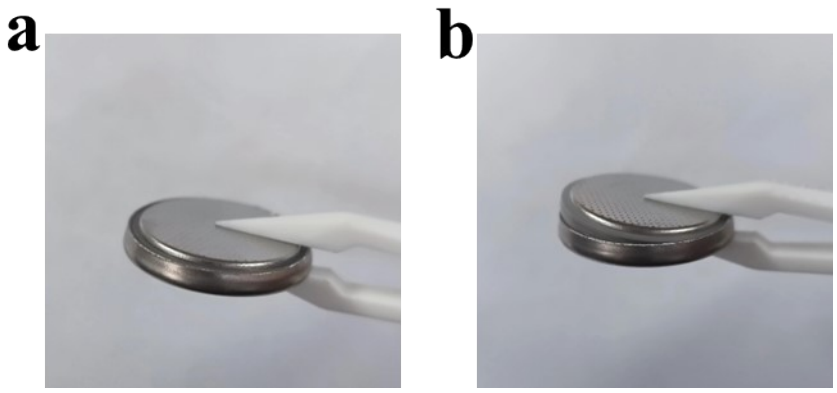

Fig. S9. Optical image of Zn//Cu asymmetric cells assembled with (a)ZFDH electrolyte and(b) ZFH electrolyte after cycling at 1 mA cm^{-2} and 0.5 mAh cm^{-2}.

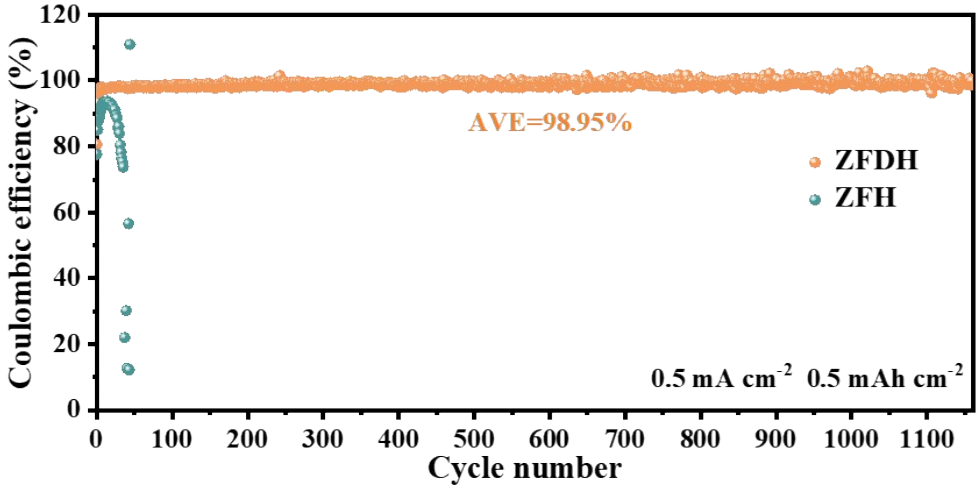

Fig. S10. Coulombic efficiency of Zn plating/stripping with ZFDH and ZFH at 0.5 mA cm^{-2} and 0.5 mAh cm^{-2}.

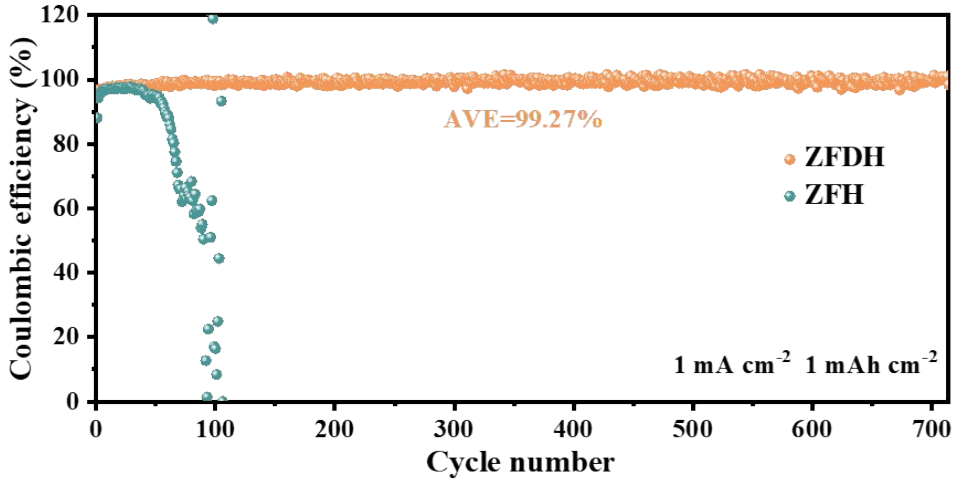

Fig. S11. Coulombic efficiency of Zn plating/stripping with ZFDH and ZFH at 1 mA cm^{-2} and 1 mAh cm^{-2}.

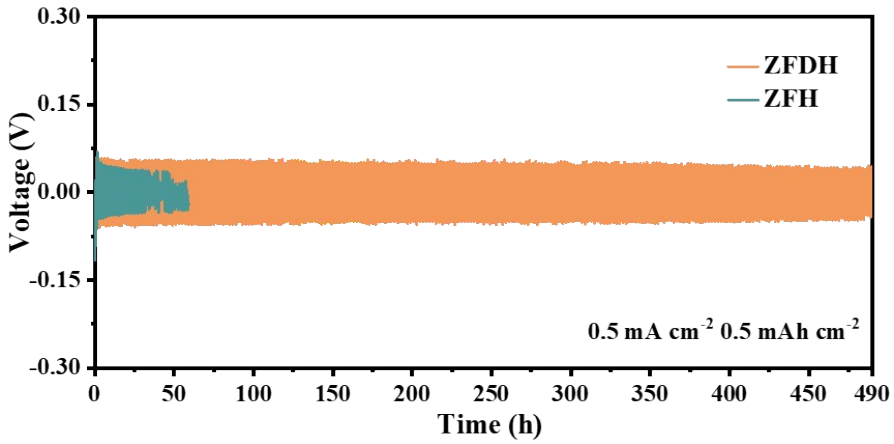

Fig. S12. Galvanostatic Zn plating/stripping in Zn//Zn symmetrical cells with ZFDH and ZFH electrolytes at 0.5 mA cm^{-2} and 0.5 mAh cm^{-2}.

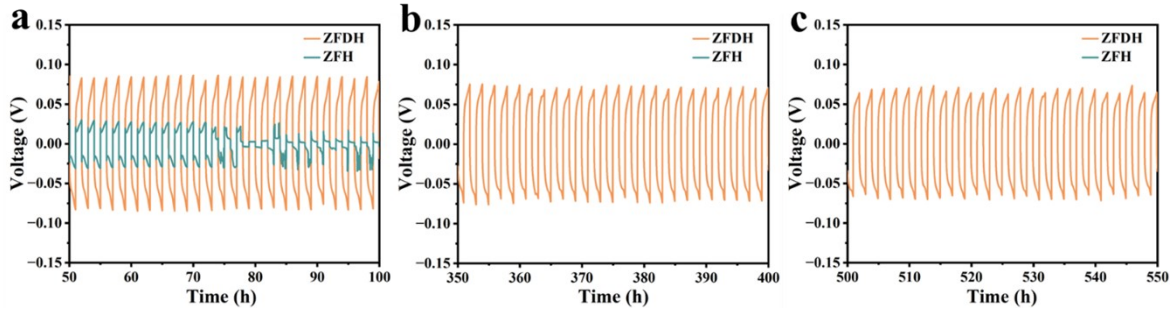

Fig. S13. The enlarged voltage profiles of Zn//Zn symmetrical cells at selected cycles at 1 mA cm^{-2} and 1 mAh cm^{-2} (a) 50-100 h; (b) 350-400 h; (c) 500-550 h.

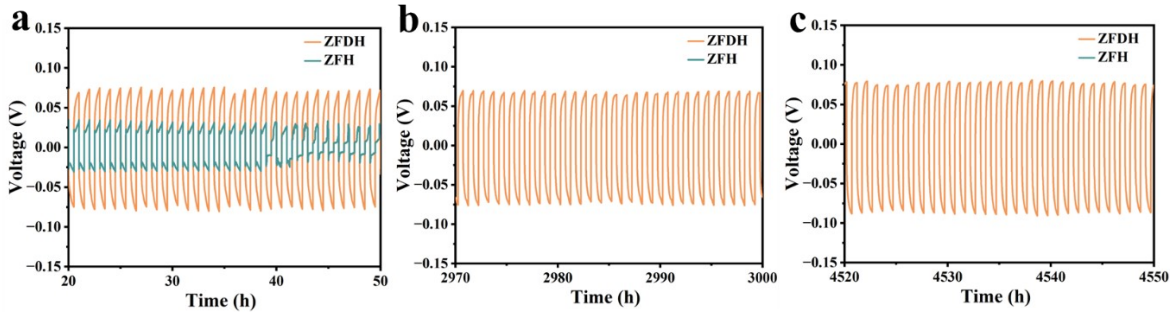

Fig. S14. The enlarged voltage profiles of Zn//Zn symmetrical cells at selected cycles at 1 mA cm^{-2} and 0.5 mAh cm^{-2} (a) 20-50 h; (b) 2970-3000 h; (c) 4520-4550 h.

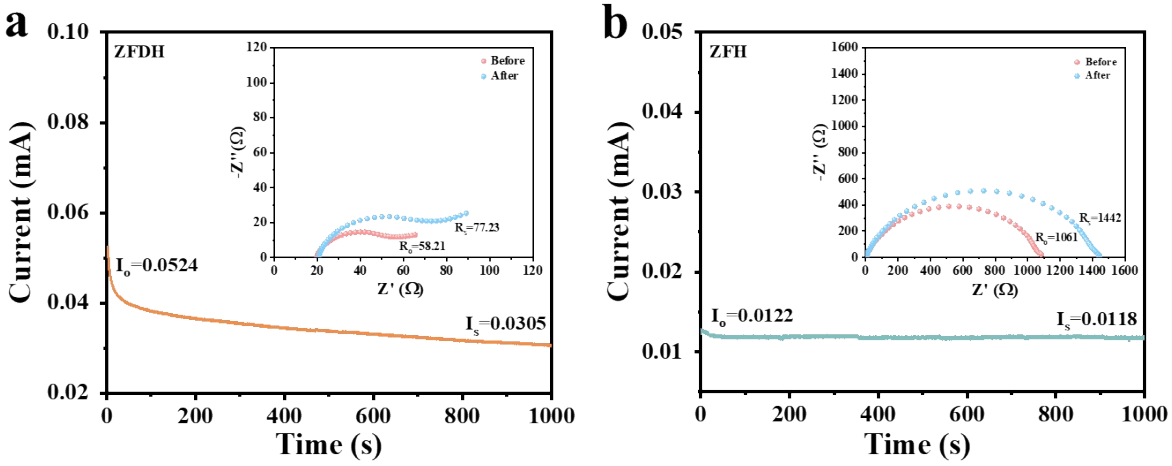

Fig. S15. Current-time plots of Zn//Zn symmetrical cells in the (a) ZFDH and (b) ZFH electrolytes after polarization at a constant potential (10 mV) for 1000 s.

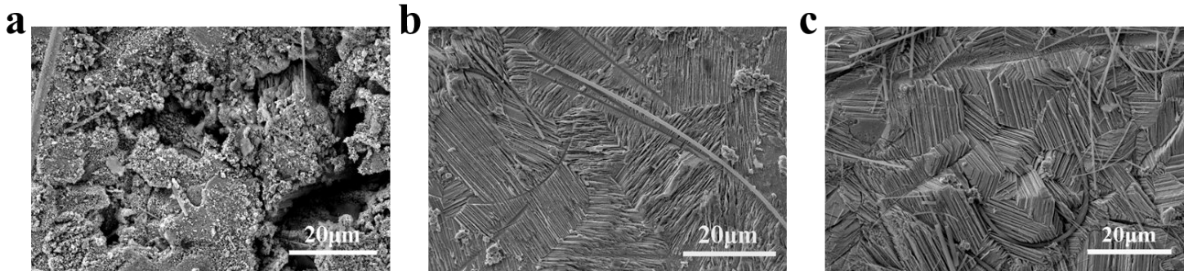

Fig. S16. SEM images of Zn electrode surface in ZFH and ZFDH electrolyte. (a) 50th cycle in ZFH (b) 50th cycle in ZFDH (c)100th cycle in ZFDH.

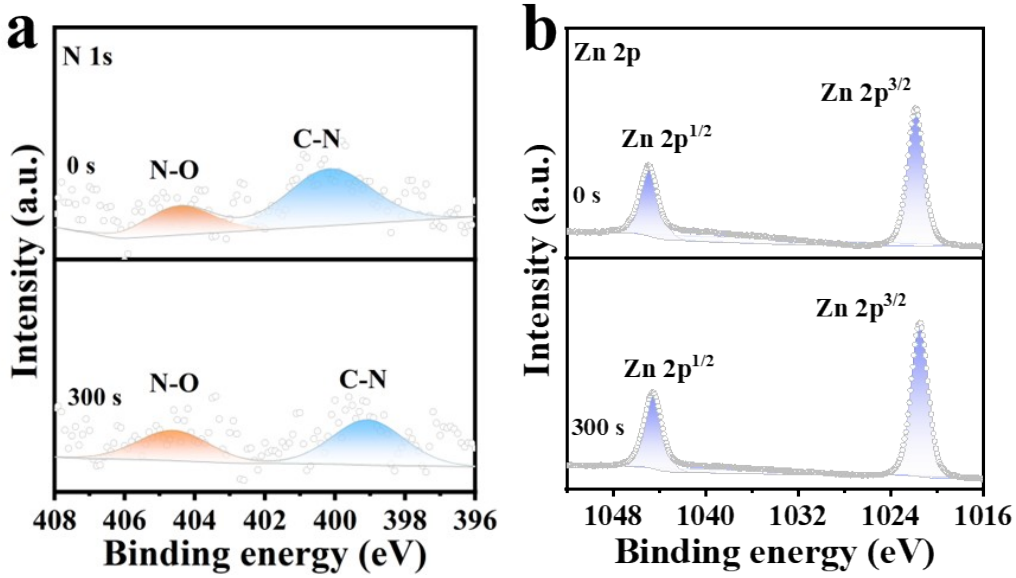

Fig. S17. XPS spectra of Zn electrode surface after cycling in the ZFDH (a) N 1s, (b) Zn 2p at different Ar^+ etching times.

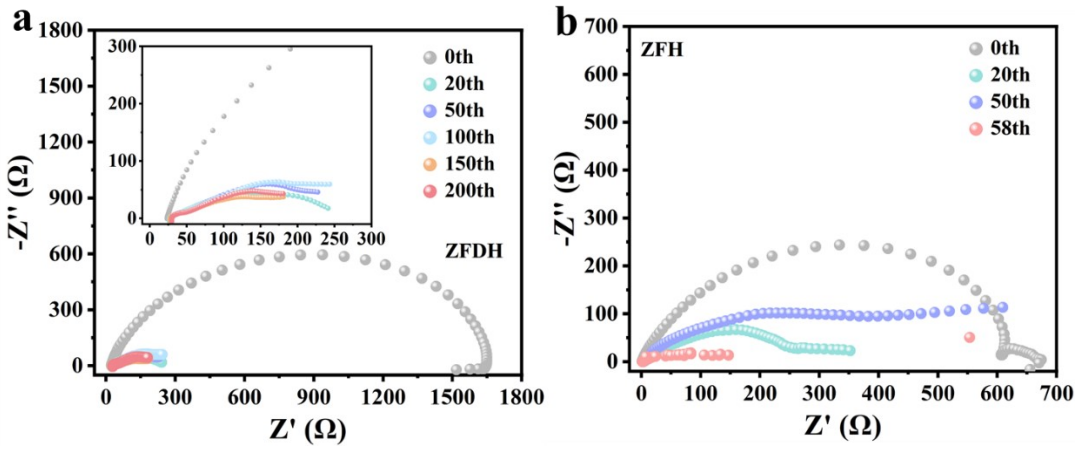

Fig. S18. EIS curves of the Zn//Zn symmetric cells after cycling for different cycles in (a) ZFDH and (b) ZFH electrolytes.

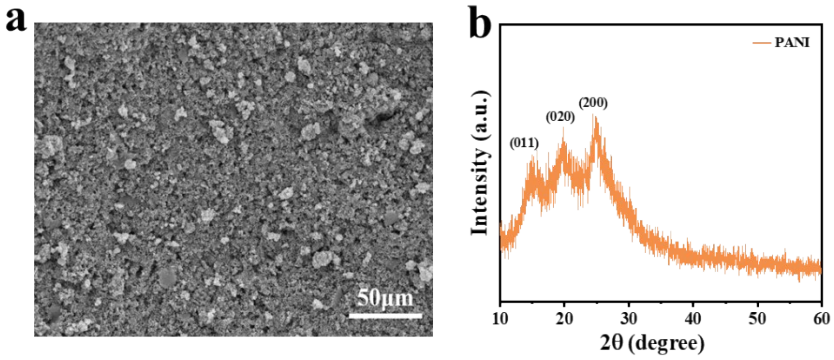

Fig. S19. SEM image, XRD pattern of PANI.

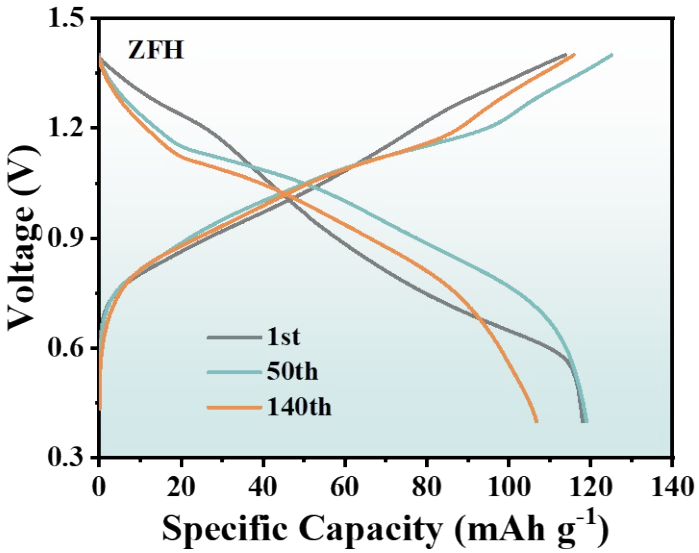

Fig. S20. Charge and discharge curves of the Zn//PANI cells with ZFH electrolytes at 0.1 A g^{-1}.

Table S1. Comparison of electrochemical performance of this work with previously

reported results.

Strategies		Current Density/ capacity (mA cm^{-2}/ mAh cm^{-2}) CE (%)	Current Density/ capacity (mA cm^{-2}/ mAh cm^{-2}) Cycle life (h)	Current density (A g^{-1}) Capacity retention (%)	dendrite suppression	Ref.
electrolyte	$ZnSO_4$+0.2NaI	1/1 97.8	10/1 864	1 67.3	Na^+ shielding layer	42
	$Zn(OTf)_2$+SL+ H_2O	2/4 99.9	2/8 1600	0.3 99.9	SEI	43
	$ZnSO_4$+MNT	1/1 97.9	1/1 2980	1 74.42	Zn (002) oriented deposition	44
	$Zn(OTf)_2$+EG+ H_2O	1/0.5 99.5	1/1 4500	1 70	/	45
	$Zn(OTf)_2$+DMI +H_2O	**1/0.5 99.72**	**1/0.5 4580**	**1 ~100**	**SEI**	**This work**
morphology modulation	5HZn-10s	1/1 97.60	11 2920	5 70.6	uniform microgroove patterns	46
	CS-Zn	1/1 97.2	2/2 3392	2 77.2	carbon nanoparticle layer	47
	3D-PBU@Zn	10/1 99.9	1/1 620	1 84.2	dual-gradient 3D porous Zn anode	48

References

1 F. Wan, L. Zhang, X. Wang, S. Bi, Z. Niu and J. Chen, *Adv. Funct. Mater.*, 2018, **7**, 1804975.

2 R. Yao, Y. Zhao, L. Wang, C. Xiao, F. Kang, C. Zhi and C. Yang, *Energy Environ. Sci.*, 2024, **17**, 3112-3122.

3 L. Geng, J. Meng, X. Wang, C. Han, K. Han, Z. Xiao, M. Huang, P. Xu, L. Zhang, L. Zhou and L. Mai, *Angew. Chem., Int. Ed.*, 2022, **134**, e202206717.

4 D. Wang, H. Peng, S. Zhang, H. Liu, N. Wang and J. Yang, *Angew. Chem., Int. Ed.*, 2023, **135**, e202315834.

5 G. J. Martyna, D. J. Tobias and M. L. Klein, *J. Chem. Phys.*, 1994, **101**, 4177–4189.

6 W. Shinoda, M. Shiga and M. Mikami, *Phys. Rev. B*, 2004, **69**, 134103.